



Pliocene and Eocene provide best analogs for near-future climates

K. D. Burke^{a,1}, J. W. Williams^b, M. A. Chandler^{c,d}, A. M. Haywood^e, D. J. Lunt^f, and B. L. Otto-Bliesner^g

^aNelson Institute for Environmental Studies, University of Wisconsin–Madison, Madison, WI 53706; ^bDepartment of Geography and Center for Climatic Research, University of Wisconsin–Madison, Madison, WI 53706; ^cCenter for Climate Systems Research, Columbia University, New York, NY 10025; ^dGoddard Institute for Space Studies, National Aeronautics and Space Administration (NASA), New York, NY 10025; ^eSchool of Earth and Environment, University of Leeds, LS2 9JT Leeds, United Kingdom; ^fSchool of Geographical Sciences, University of Bristol, BS8 1SS Bristol, United Kingdom; and ^gClimate and Global Dynamics Laboratory, National Center for Atmospheric Research, Boulder, CO 80305

Edited by Noah S. Diffenbaugh, Stanford University, Stanford, CA, and accepted by Editorial Board Member Robert E. Dickinson November 6, 2018 (received for review June 29, 2018)

As the world warms due to rising greenhouse gas concentrations, the Earth system moves toward climate states without societal precedent, challenging adaptation. Past Earth system states offer possible model systems for the warming world of the coming decades. These include the climate states of the Early Eocene (ca. 50 Ma), the Mid-Pliocene (3.3–3.0 Ma), the Last Interglacial (129–116 ka), the Mid-Holocene (6 ka), preindustrial (ca. 1850 CE), and the 20th century. Here, we quantitatively assess the similarity of future projected climate states to these six geohistorical benchmarks using simulations from the Hadley Centre Coupled Model Version 3 (HadCM3), the Goddard Institute for Space Studies Model E2-R (GISS), and the Community Climate System Model, Versions 3 and 4 (CCSM) Earth system models. Under the Representative Concentration Pathway 8.5 (RCP8.5) emission scenario, by 2030 CE, future climates most closely resemble Mid-Pliocene climates, and by 2150 CE, they most closely resemble Eocene climates. Under RCP4.5, climate stabilizes at Pliocene-like conditions by 2040 CE. Pliocene-like and Eocene-like climates emerge first in continental interiors and then expand outward. Geologically novel climates are uncommon in RCP4.5 (<1%) but reach 8.7% of the globe under RCP8.5, characterized by high temperatures and precipitation. Hence, RCP4.5 is roughly equivalent to stabilizing at Pliocene-like climates, while unmitigated emission trajectories, such as RCP8.5, are similar to reversing millions of years of long-term cooling on the scale of a few human generations. Both the emergence of geologically novel climates and the rapid reversion to Eocene-like climates may be outside the range of evolutionary adaptive capacity.

climate change | climate analog | no analog | paleoclimate | planetary boundary

By the end of this century, mean global surface temperature is expected to rise by 0.3 °C to 4.8 °C relative to 1986–2005 CE averages, with more warming expected for higher levels of greenhouse gas emissions (1) and substantial effects predicted for the cryospheric (2), hydrologic (3), biological (4, 5), and anthropogenic (6) components of the Earth system. Understanding and preparing for climate change are challenged in part by the emergence of Earth system states far outside our individual, societal, and species' experience. Traditional systems for designing infrastructure, mitigating natural hazard risk, and conserving biodiversity are often based on implicit assumptions about climate stationarity and recent historical baselines (7), which fail to encompass expected trends and recent extreme events (8, 9). Calls to keep the Earth within a “safe operating space” seek to keep Earth's climates in the range of those experienced during the Holocene, which encompasses the time of development of agriculture and the emergence of the complexly linked global economy (10, 11). Societally novel climates are expected to emerge first in low-latitude and low-elevation regions (12–14), while locally novel climates (future climates that have exceeded a baseline of local historical variability) are expected to begin to emerge by the mid- to late 21st century (15–17).

However, all prior efforts to quantify the pattern and timing of novel climate emergence have been narrowly restricted to shallow

baselines, in which the 20th and 21st century instrumental records are used for reference. This restriction overlooks the deep history of Earth's climate variation and the societal, ecological, and evolutionary responses to this past variation. By considering only shallow temporal baselines, the evolutionary adaptive capacity of species to future novel climates may be underestimated. Conversely, others have drawn informal analogies between the climates of the future and those of the geological past (18, 19), but there has been no quantitative comparison. Here, we pursue a deeper baseline, formally comparing the projected climates of the coming decades with geohistorical states of the climate system from across the past 50 My. We seek to identify past states of the climate system that offer the closest analogs to the climates of the coming decades, the time to emergence for various geological analogs, and the distribution and prevalence of “geologically novel” future climates (i.e., that lack any close geological analog among the climate states considered here).

Identifying the Closest Paleoclimatic Analogs for Near-Future Earth

Earth's climate system has evolved in response to external forcings and internal feedbacks across a wide range of timescales (Fig. 1). Since 65 Ma, global climate has cooled (20), and

Significance

The expected departure of future climates from those experienced in human history challenges efforts to adapt. Possible analogs to climates from deep in Earth's geological past have been suggested but not formally assessed. We compare climates of the coming decades with climates drawn from six geological and historical periods spanning the past 50 My. Our study suggests that climates like those of the Pliocene will prevail as soon as 2030 CE and persist under climate stabilization scenarios. Unmitigated scenarios of greenhouse gas emissions produce climates like those of the Eocene, which suggests that we are effectively rewinding the climate clock by approximately 50 My, reversing a multimillion year cooling trend in less than two centuries.

Author contributions: K.D.B. and J.W.W. designed research; K.D.B. performed research; K.D.B., J.W.W., M.A.C., A.M.H., D.J.L., and B.L.O.-B. analyzed data; M.A.C., A.M.H., D.J.L., and B.L.O.-B. contributed climate model simulation data; and K.D.B., J.W.W., M.A.C., A.M.H., D.J.L., and B.L.O.-B. wrote the paper.

The authors declare no conflict of interest.

This article is a PNAS Direct Submission. N.S.D. is a guest editor invited by the Editorial Board.

Published under the PNAS license.

Data deposition: The Matlab code used to identify closest analogs as well as the output files, which contain the geographic information, climatic distances, and analog matches, have been deposited in the Dryad Digital Repository (doi.org/10.5061/dryad.0j18k00).

¹To whom correspondence should be addressed. Email: kdburke@wisc.edu.

This article contains supporting information online at www.pnas.org/lookup/suppl/doi:10.1073/pnas.1809600115/-DCSupplemental.

Published online December 10, 2018.

atmospheric CO₂ concentrations have declined (21). Several warm periods offer possible geological analogs for the future: the Early Eocene (ca. 50 Ma; hereafter the Eocene), the Mid-Pliocene Warm Period (3.3–3.0 Ma; hereafter the Mid-Pliocene), the Last Interglacial (LIG; 129–116 ka), and the Mid-Holocene (6 ka). During the Eocene, the warmest sustained state of the Cenozoic, global mean annual surface temperatures were 13 °C ± 2.6 °C warmer than late 20th century temperatures (22), there was no permanent ice, and atmospheric CO₂ was approximately 1,400 parts per million volume (ppmv) (23). The Mid-Pliocene is the most recent period with atmospheric CO₂ comparable with the present (ca. 400 ppmv) (24), with mean annual surface temperatures approximately 1.8 °C to 3.6 °C warmer than preindustrial temperatures, reduced ice sheet extents, and increased sea levels (25). During the LIG, global mean annual temperatures were approximately 0.8 °C (maximum 1.3 °C) warmer than preindustrial temperatures (26), and amplified seasonality characterized the northern latitudes (27). During the Mid-Holocene, temperatures were 0.7 °C warmer than preindustrial temperatures (28), with enhanced temperature seasonality and strengthened Northern Hemisphere (NH) monsoons (27).

Recent historical intervals also provide potential analogs for near-future climates (Fig. 1), including preindustrial climates (ca. 1850 CE) and a mid-20th century snapshot (1940–1970 CE). The preindustrial era represents the state of the climate system before the rapid acceleration of fossil fuel burning and greenhouse gas emissions, while the mid-20th century (“historical”) snapshot represents the center of the meteorological instrumental period that is the foundation for most societal estimates of climate variability and risk.

Here, we formally compare projected climates for the coming decades with these six potential geohistorical analogs (Fig. 1) using climate simulations produced by Earth system models (ESMs). We focus on two Representative Concentration Pathways (RCPs), RCP4.5 and RCP8.5, and find geohistorical analogs for projected climates for each decade from 2020 to 2280 CE. We analyze simulations for three ESMs with simulations available for the past and future periods considered here: the Hadley Centre Coupled Model Version 3 (HadCM3), the Goddard Institute for Space Studies Model E2-R (GISS), and the Community Climate System Model, Versions 3 and 4 (CCSM) (SI Appendix, Tables S1 and S2). To assess the similarity between future and past climates, we calculate the Mahalanobis distance (MD) based on a four-

variable vector of mean summer and winter temperatures and precipitation (*Materials and Methods*). The climate for each terrestrial grid location for a given future decade is compared with all points in a reference baseline dataset that comprises the climates of all global terrestrial grid locations from all six geohistorical periods (SI Appendix, Figs. S1 and S2). For each location, we identify for each future climate its closest geohistorical climatic analog (i.e., the past time period and location with the most similar climate). We apply this global similarity assessment to each future decade from 2020 to 2280 CE. Future climates that exceed an MD threshold are classified as “no analog” (*Materials and Methods*), indicating that they lack any close analog in the suite of geological and historical climates considered here.

Results

Historical climates and preindustrial climates quickly disappear as best analogs for 21st century climates for both RCP scenarios (Fig. 2). By 2040 CE, they are replaced by the Mid-Pliocene, which becomes the most common source of best analogs in the three-model ensemble and remains the best climate analog thereafter (Fig. 2). Hence, RCP4.5 is most akin to a Pliocene commitment scenario, with the planet persisting in a climate state most similar to that of the Mid-Pliocene (Fig. 2). However, the preindustrial and historical baselines remain among the top three closest analogs for RCP4.5 throughout the entire 2020–2280 period (providing 18.1 and 16.8% of analogs at 2280 CE, respectively), while the Mid-Holocene and the LIG provide 16.2 and 10.1% of matches, respectively, at 2280 CE. Among individual models, the Mid-Pliocene is consistently one of the best analogs for RCP4.5 climates, but its prevalence and the ranking of the other geohistorical analogs tested vary among models (Fig. 2).

Conversely, for the RCP8.5 ensemble, the Eocene emerges as the most common best analog (Fig. 2). The Mid-Pliocene becomes the best climate analog slightly sooner, by 2030 CE, but the prevalence of Eocene-like climates accelerates after 2050 CE, and future climates most commonly resemble the Eocene by 2140 CE. The historical and preindustrial time periods remain best analogs only briefly until 2030 CE. The switch to Eocene-like climates occurs as early as 2130 CE (HadCM3) and remains a close second until 2280 with GISS. Across all models, the proportion of future climates with best matches

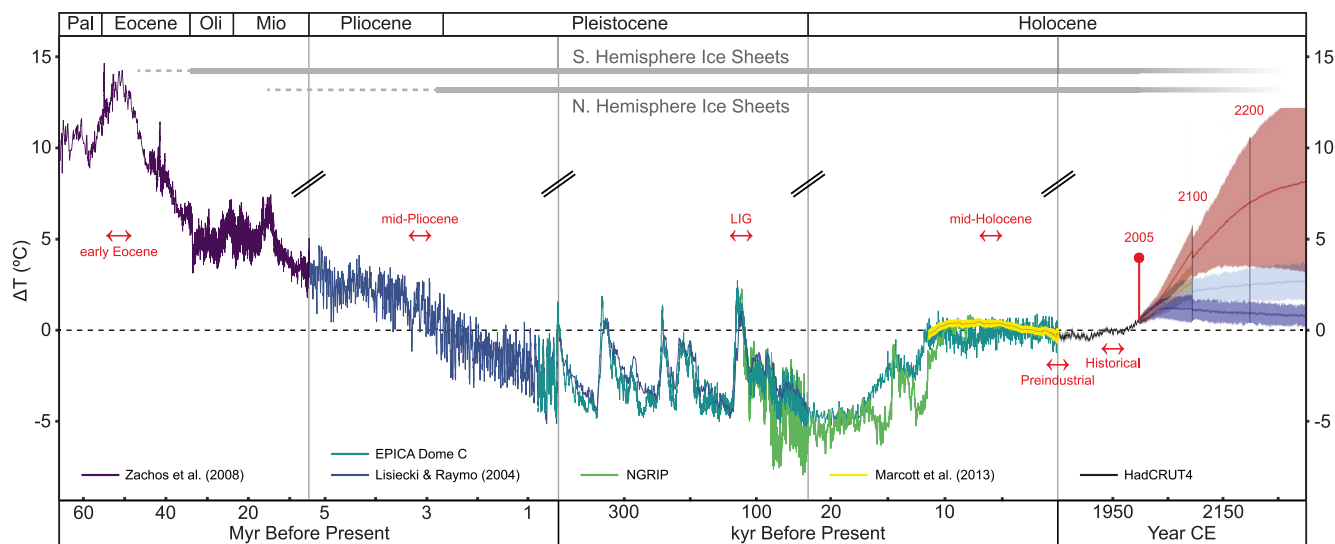


Fig. 1. Temperature trends for the past 65 Ma and potential geohistorical analogs for future climates. Six geohistorical states (red arrows) of the climate system are analyzed as potential analogs for future climates. For context, they are situated next to a multi-timescale time series of global mean annual surface temperatures for the last 65 Ma. Major patterns include a long-term cooling trend, periodic fluctuations driven by changes in the Earth’s orbit at periods of 10⁴–10⁵ y, and recent and projected warming trends. Temperature anomalies are relative to 1961–1990 global means and are composited from five proxy-based reconstructions, modern observations, and future temperature projections for four emissions pathways (*Materials and Methods*). Pal, Paleocene; Mio, Miocene; Oli, Oligocene.

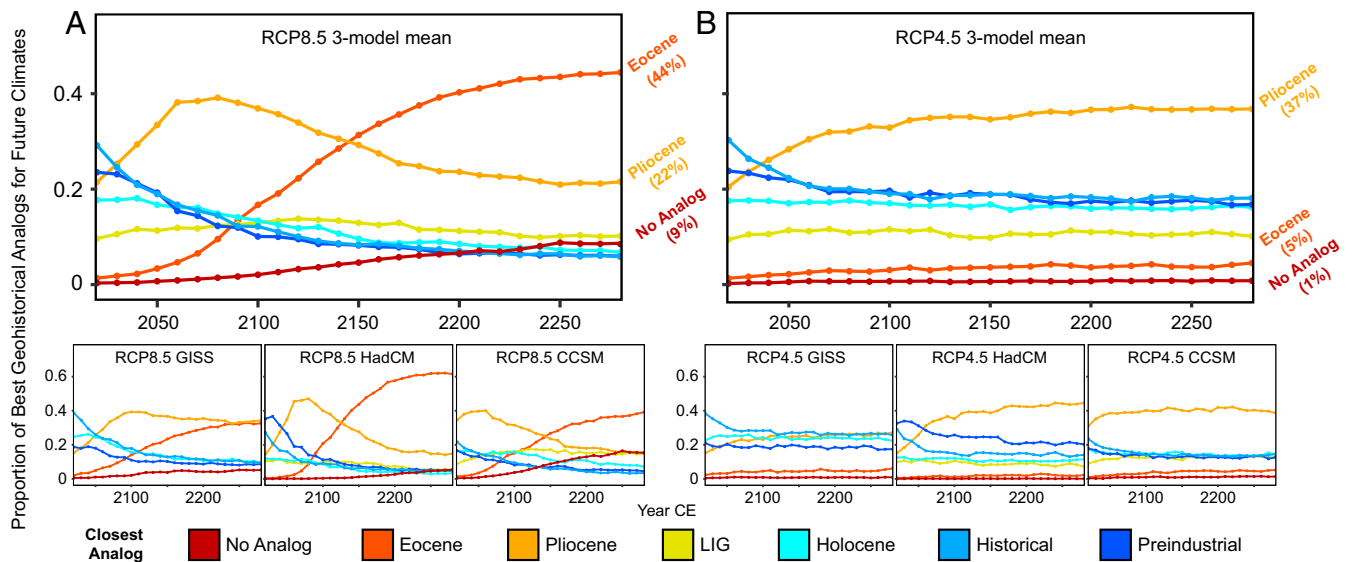


Fig. 2. Time series of the closest geohistorical climatic analogs for projected climates, 2020–2280 CE (MD). Colored lines indicate the proportion of terrestrial grid cells for each future decade with the closest climatic match to climates from six potential geohistorical climate analogs: Early Eocene, Mid-Pliocene, LIG, Mid-Holocene, preindustrial, and historical for RCP8.5 (A) and RCP4.5 (B). No LIG simulation from GISS was available at the time of analysis.

to the Eocene increases to 44.4% at 2280 CE. Other potential analogs for RCP8.5 climates at 2280 CE include the Mid-Pliocene and LIG (21.6 and 10.2%).

Under RCP8.5, the percentage of geologically novel future climates steadily increases. By 2100 CE, 2.1% of projected climates are geologically novel (0.4% HadCM3, 2.1% GISS, and 3.8% CCSM). By 2280 CE, the ensemble prevalence of geologically novel climates increases to 8.7% (5.4% HadCM3, 5.2% GISS, and 15.3% CCSM) (*SI Appendix, Table S3*). Conversely, geologically novel climates are uncommon for RCP4.5, with <1.5% of locations with no analog to any past climate simulation, across all models and all decades.

By 2030 CE under RCP8.5, continental interiors are the first to reach Pliocene-like climates (Fig. 3 and *SI Appendix, Fig. S3* for individual models and *SI Appendix, Fig. S4* for RCP4.5), with LIG analogs also common in CCSM in the NH midlatitudes. In subsequent decades, Mid-Pliocene-like climates spread outward from their regions of origin (*Movies S1–S8*). Changes between 2050 and 2100 CE are striking (Fig. 3 and *SI Appendix, Fig. S3*), with Mid-Pliocene matches widespread and Eocene matches emerging in continental interiors by 2100 CE. By 2100 CE, matches to historical and preindustrial climates are uncommon and mostly found in Arctic locations that are drawing best analogs from far to the south (*SI Appendix, Fig. S13*)—the last to leave societally familiar climate space. After 2200 CE, the Early Eocene becomes the most common source of climate matches across all continents and models. The 23rd century is also characterized by the onset of geologically novel climates concentrated in eastern and southeastern Asia, northern Australia, and coastal Americas (Fig. 3 and *SI Appendix, Fig. S3*).

Rapidly rising temperatures are the primary reason that future climate matches are drawn from increasingly distant time periods (Fig. 4 and *SI Appendix, Fig. S5*). As the world warms, locations near the leading edge of climate space first resemble the Mid-Pliocene, but additional warming pushes them toward the Early Eocene or geologically novel climates (i.e., novel relative to the past time periods considered here). Climate matches to the LIG cluster along the leading edge of T_{JJA} space, likely due to warming and heightened boreal thermal seasonality during the LIG, which makes these climates good analogs for future high-latitude climates (27). Geologically novel climates tend to be characterized by high temperature and precipitation (Fig. 4) and are associated with monsoonal climates or locations near the intertropical convergence zone (Fig. 3).

These analyses are based on past and future ESM simulations, which contain uncertainties in forcing and model specification, some data–model mismatches, and other areas of ongoing improvement (29, 30). Our results are dependent on the climate states included in our geohistorical reference baseline and could change if additional climate states were included. However, given that the Eocene is the warmest sustained state of the entire Cenozoic, if a future state is novel, it is likely novel at least relative to any Cenozoic climate state. Despite these caveats, these simulations represent the most complete realization available of past and future global climate states. These models and geohistorical climate scenarios that were chosen have been intensively studied and validated, including model intercomparisons (25, 27, 31) and model–data studies (32, 33).

Discussion

These analyses illustrate how the policy and societal choices represented by RCP emission scenarios are akin to choosing a geological analog, with higher-end scenarios causing near-future climates to resemble increasingly distant geological analogs. For RCP8.5, the emergence of Eocene-like climates indicates that the unmitigated warming of RCP8.5 is approximately equivalent to reversing a 50-My cooling trend in two centuries. Conversely, stabilization pathways, such as RCP4.5, are akin to choosing a world like the Mid-Pliocene (ca. 3 Ma).

These analyses also indicate that the Earth system is well along on a trajectory to a climate state different from any experienced in our history of agricultural civilizations (last 7 ka) (34) and modern species history (360–240 ka) (35). Climate states for which we have good historical and lived experience (e.g., 20th century, preindustrial) are quickly diminishing as best analogs for the coming decades, while being superseded by climate analogs drawn from deeper times in Earth’s geological history (Figs. 2 and 3). Future climates also tend to exhibit greater geographic separation from their closest analogs over the coming centuries (*SI Appendix, Fig. S14*). Efforts to keep the Earth within a safe operating space, defined as climates similar to those of the Holocene (11, 36), seem to be increasingly unlikely.

However, most future climates do carry geological precedents, which provide grounds for both hope and concern. The prevalence of future novel climates in these analyses (Figs. 2 and 3) is far lower than in prior studies (13, 14), because the deeper baselines used here encompass a broader range of climate states than for analyses based on shallow baselines that comprise only 20th and

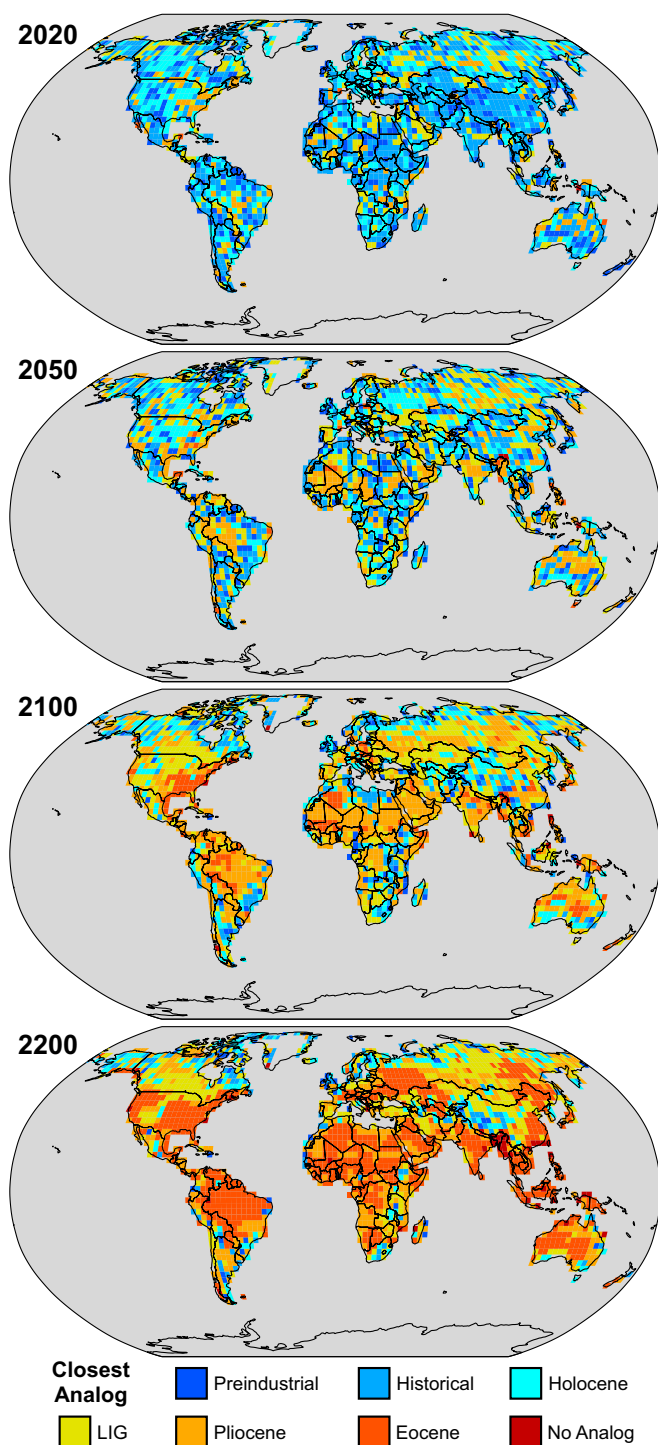


Fig. 3. Projected geographic distribution of future climate analogs (RCP8.5). Future climate analogs for 2020, 2050, 2100, and 2200 CE according to the ensemble median. Geohistorical periods are rank ordered according to global mean annual temperature as follows: preindustrial, historical, Mid-Holocene, LIG, Pliocene, and Eocene, with no analog placed at the end due to the prevalence of no-analog climates in the warmest and wettest portion of climate space (Fig. 4). Hence, a projected future location matched to Pliocene, Eocene, and no analog in the three ESMs would be identified as Eocene in the ensemble median.

early 21st century climates (Fig. 1). Conversely, the novel climates identified here carry greater import, because they highlight regions where projected climates lack any close analog among the

geohistorical climate states considered here. These analyses underscore the utility of Earth's history as a series of natural experiments for understanding the responses of physical and biological systems to large environmental change (37, 38). The availability of geological analogs to future climates also offers some evidence for ecoevolutionary adaptive capacity in that most future climates have equivalents in the deep evolutionary histories of current lineages. All species present today have an ancestor that survived the hothouse climates of the Eocene and Pliocene.

However, these analyses also raise serious concerns about adaptive capacity. The large climate changes expected for the coming decades will occur at a significantly accelerated pace compared with Cenozoic climate change and across a considerably more fragmented landscape, rife with additional stresses. Over the past 50 My, evolutionary changes have been driven in part by species adapting away from hothouse climates to a world that was cooling, drying, and characterized by decreasing atmospheric CO₂. For example, the rise of C₄ grasslands, grazing specialists, and other evolutionary changes during the Miocene (Mio) and the Pliocene are linked to increasing aridity, decreasing CO₂, and rising temperatures (39). Thermophilous tree species in Europe seem to have been driven to extinction by Pliocene cooling and Quaternary glacial periods (40). The rates of temperature increases expected this century are at the high end of those recorded in geological history, with well-established counterparts only in the abrupt millennial-scale climate variations in the North Atlantic and adjacent regions during the last glacial period (41). Based on thermodynamic first principles, rising heat energy in the atmosphere–ocean system is expected to increase the frequency or intensity of extreme events (42) that are critical controls on species distributions and diversity. High rates of change is a defining feature of the emerging Anthropocene and a key difference between the climates of the near future and those of the geohistorical past.

Materials and Methods

Past and Future Climate Simulations. A growing catalog of global climatic experiments with ESMs enables quantitative comparisons of future climate projections with potential analogs drawn from across Earth's history. Since ESMs are computationally expensive, most paleoclimatic experiments are snapshot-style simulations (10²–10⁴ y) run for a sufficiently long time that trends in global mean surface temperature are small. They are used to study the climate response to forcings and feedbacks (e.g., Earth orbital variations, greenhouse gas concentrations) or understand particular phenomena (e.g., reduced zonal and meridional temperature gradients). Formal model intercomparison projects (27, 31, 43) prescribe common boundary conditions for paleoclimatic simulations. The six geohistorical time periods used here have all been the subject of multiple model–model and data–model comparisons (44, 45).

Similarly configured ESMs are used to simulate Earth system responses to future scenarios of rising radiative forcings associated with greenhouse gas concentrations (46). RCP4.5 and RCP8.5 are transient scenarios of rising radiative forcing associated with changes in greenhouse gas emissions and atmospheric composition. RCP4.5 represents a stabilization of radiative forcing at 4.5 W/m² and CO₂ concentrations of approximately 550 ppmv by 2100 CE (47). RCP8.5 is characterized by high greenhouse gas emissions, resulting in an increase in radiative forcing of 8.5 W/m² and CO₂ concentrations of approximately 1,000 ppmv by 2100 CE relative to the preindustrial (48). Beyond 2100 CE, RCP4.5 is extended assuming concentration stabilization in 2150 CE, and RCP8.5 is extended assuming constant emissions after 2100 CE followed by a smooth transition to stabilized concentrations after 2250 CE (46). Thus, RCP4.5 corresponds to an approximately 4.5 W/m² total increase in radiative forcing by 2280 CE, while RCP8.5 corresponds to an approximately 12 W/m² total increase. The atmospheric CO₂ concentrations for 2280 CE correspond to approximately 550 and 2,000 ppmv, respectively.

We use a three-ESM ensemble (HadCM3, GISS, CCSM) to assess the similarity of future and past climates and identify best analogs. Analyses are conducted only within model family (e.g., future projections from the CCSM model are compared only with past CCSM simulations), because standard bias correction is not possible due to changes in paleogeography. For all past and future simulations, we create a standard climatology (typically a 30-y mean), with means calculated for four indicator variables: 1.5 m air temperature for December, January, and February (T_{DJF}); 1.5 m air temperature for June, July, and August (T_{JJA}); and total monthly precipitation for these two seasons

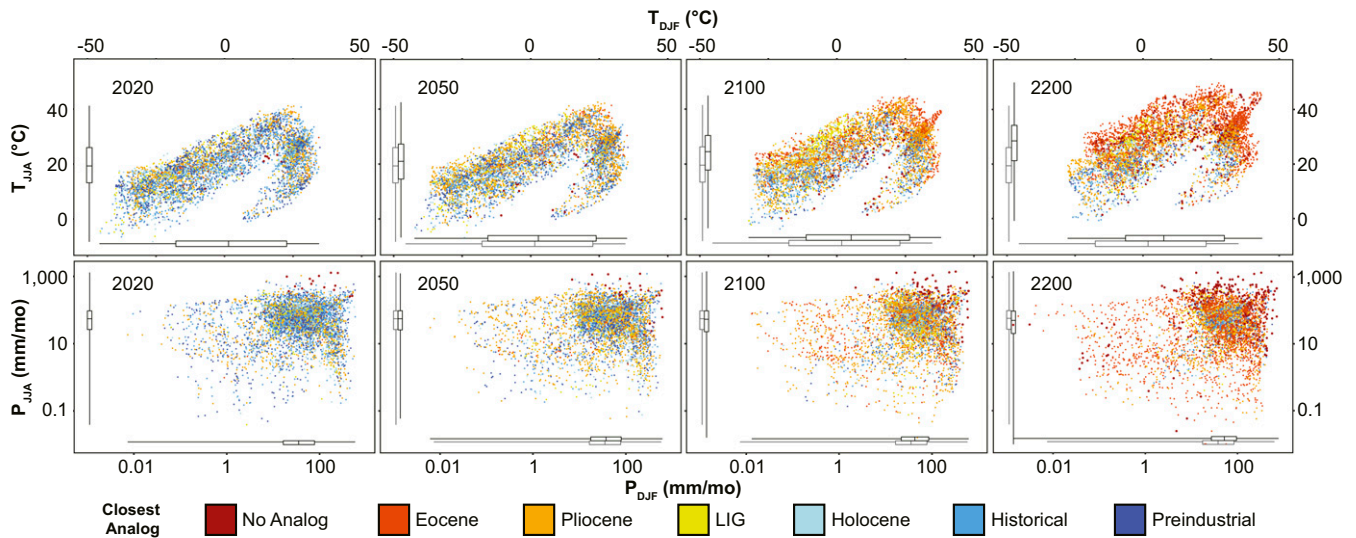


Fig. 4. Projected future climate space by closest analog (RCP 8.5). (Upper) DJF vs. JJA temperature space. (Lower) DJF vs. JJA precipitation space. Each point represents a terrestrial grid location from the model ensemble for the specified decade in the RCP8.5 projection. Points are color coded according to the geohistorical climate from which their closest analog sources. Box-and-whisker plots show the data range, median, and first and third quartiles for two time periods: the specified decade (black) and 2020 CE for reference (gray).

(P_{DJF} and P_{JJA} , respectively). We apply a land–sea mask and an ice mask to restrict the analyses to terrestrial grid cells that are not covered by permanent ice. Simulations were bilinearly interpolated to a common T42 spatial resolution (128 cells longitude \times 64 cells latitude; ca. 2.79° at the equator). Before regridding, individual simulations ranged from (72 \times 46) to (288 \times 192), with higher resolution typically associated with projections of future climate (SI Appendix, Table S1).

We analyzed future climate projections for every decade between 2020 and 2280 CE, producing a future climate dataset of approximately 1,900 locations \times 27 decades. Each decade is the center of a 30-y climatology; therefore, the entire dataset spans 2005–2295 CE, and individual decadal climatologies overlap their neighbors. The pool of potential past climate scenarios comprises 12,576 focal cells across the six past time periods for the HadCM3, 13,213 for the CCSM, and 10,483 for the GISS (for which no LIG simulation was available at time of this analysis). When multiple ensemble members were available, the first ensemble member was used.

Climate Similarity Analyses. We apply the MD metric to quantify multivariate dissimilarity for future projections of climate using a four-variable vector of DJF and JJA temperature and precipitation. MD is calculated for each future climate point (i.e., for a given grid location and decade) relative to all points in a reference baseline of past climates that comprise the climates at all terrestrial grid locations across all geohistorical time periods. MD is calculated as follows:

$$MD_{ij} = \sqrt{(\vec{b}_j - \vec{a}_i)^T S^{-1} (\vec{b}_j - \vec{a}_i)},$$

where a_i refers to a vector of indicator variables ($n = 4$) from focal cell i of the reference baseline dataset, b_j refers to a vector of indicator variables from focal cell j of the period for which dissimilarity is being assessed, and S^{-1} is the covariance matrix of the data estimated from the future and reference climatologies. For each future point, we conduct a series of one-to-many comparisons, where the similarity of each future point is compared with all points in the reference baseline. The past climate point with the minimum MD to the target future climate point is defined as the closest analog. Hence, the past analog can be drawn from any spatiotemporal location, and its selection is based only on climate similarity. See SI Appendix, Fig. S2 for an example location in Eurasia.

The choice of multivariate distance metric and variables for climate similarity analyses has received increasing attention in recent years. Standardized Euclidean distance (SED) has been the standard (12, 13), although other metrics, including MD and sigma dissimilarity (14), have gained prominence. These metrics are appealing, because they consider the correlation structure among variables and down weight highly correlated variables. Here, we use MD for the primary analyses but also apply the SED metric as an alternative

approach for quantifying multivariate dissimilarity (SI Appendix, Figs. S6 and S7). Its calculation is as follows:

$$SED_{ij} = \sqrt{\sum_{k=1}^n \frac{(b_{kj} - a_{ki})^2}{s_k^2}},$$

where k indexes the climate variables ($n = 4$), s_k refers to the SD of variable k , and other variables are consistent with MD above. Dividing each variable by its variance seeks to standardize the values to a common scale. Hence, the calculated difference $b_{kj} - a_{ki}$ is only important if it is large relative to s_k . Due to the lack of availability of annually simulated climate values for all time periods, we use a modern estimate of interannual variability from 1960 to 1990 CE from the observational Climate Research Unit dataset (CRU TS 3.23) (49) for s_k . Focal cells, where s_k is zero for at least one variable, are mapped as NA (this happens when precipitation has a value of zero for the entire 30-y climatology). Results are generally similar between the MD and SED metrics, but the SED analyses indicate a slightly earlier arrival of Pliocene-like climates and greater prevalence of geologically novel climates (SI Appendix, Fig. S6).

Experiments basing climate similarity on two vs. four seasons suggest little effect on novelty (14). Conversely, the use of average annual temperature rather than seasonal minima and maxima tends to reduce the true dimensionality of climate space and underestimate the prevalence of novel climates (14). Hence, by defining climate as a vector of seasonal temperature and precipitation means, we balance the selection of climatic dimensions important to species distribution and diversity (50) with the availability of simulated climate data (30). Minimum and maximum monthly temperature estimates were unavailable for all model simulations included in our analyses. Our inclusion of four indicator variables, therefore, offers the best available assessment of climate analogs and novelty for our study design.

Novel Climate Threshold. No-analog climates are defined as best-analog matches with MD values that exceed a prescribed threshold. Here, the no-analog threshold is defined as the 99th percentile of MD or SED values from the population of modern (1970–2000 CE) climates matched to their best analogs in preindustrial climates (SI Appendix, Fig. S11). As such, the climate of a focal location is different beyond nearly any distance that a modern location would exhibit compared with a preindustrial baseline.

Paleotemperature Time Series. Fig. 1, used here to illustrate the evolution of the Earth's climate system over the past 65 My (but not as the basis of any quantitative climate similarity analyses), includes five proxy-based temperature reconstructions (28, 51–54), a modern observational data product (55), and future temperature projections following four radiative concentration pathways (1). The benthic $\delta^{18}O$ values were first converted to deep sea

temperature approximations and then to surface temperature approximations (56). The European Project for Ice Coring in Antarctica (EPICA) and North Greenland Ice Core Project (NGRIP) temperature anomalies are presented relative to the last millennium and core top, respectively, and assume a polar amplification factor of two. The Holocene temperature reconstruction shows the $5^\circ \times 5^\circ$ area-weighted global mean temperature anomaly $\pm 1\sigma$. The Hadley Centre and Climatic Research Unit Temperature dataset, v. 4 (HadCRUT4) observational data product shows the $5^\circ \times 5^\circ$ ensemble median and 95% confidence interval of the combined effects of all of the uncertainties described in the HadCRUT4 error model. Projected temperature anomalies after 2005 CE correspond to RCP scenarios 2.6, 4.5, 6.0, and 8.5. Solid lines correspond to multimodel means, and shading corresponds to the 5–95% model range. Discontinuities at 2100 CE are caused by a change in the number of models included in the ensemble. Projected temperature anomalies for RCP scenarios were shifted $+0.3^\circ\text{C}$ to account for warming between the 1961–1990 and 1986–2005 CE reference periods used for the paleoclimatic time series and RCP scenarios, respectively (see ref. 1, table 12.2). Scaling of time varies among five panels to illustrate major features of the Earth's climate history at different timescales. Geologic ages are expressed relative to 1950 CE. All climate similarity analyses are based on the paleoclimate and 21st century climate simulations from HadCM3, GISS, and

CCSM. Figure design is modified from ref. 57 and (https://en.wikipedia.org/wiki/File:All_palaetemps.png).

Future Climate Space Mapped by Closest Past Climate Scenario. Plotting of future climates with respect to climate axes (Fig. 4 and *SI Appendix, Fig. S5*) shows how the global distribution of realized climates changes over the coming decades, with colors indicating the shifting sources of best geohistorical analogs. Due to changes in model forcings, future climate generally warms. Precipitation patterns are less unidirectional, with some regions warming and others drying.

ACKNOWLEDGMENTS. We acknowledge the World Climate Research Programme and Coupled Model Intercomparison Project, the Paleoclimate Modeling Intercomparison Project, the Earth System Grid, the Bristol Research Initiative for the Dynamic Global Environment, M. J. Carmichael, A. Farnsworth, P. J. Valdes, and L. E. Sohl for assistance in obtaining climate simulation data. We thank V. C. Radeloff, C. R. Mahony, A. J. Jacobson, Y. Liu, members of the J.W.W. laboratory, and the Novel Ecosystems Integrative Graduate Education and Research Traineeship participants (1144752) for thoughtful discussion during manuscript development. Additional support was provided by NSF Grant DEB-1353896, NSF sponsorship of National Center for Atmospheric Research, as well as the Wisconsin Alumni Research Foundation.

- IPCC (2013) *Working Group I Contribution to the IPCC Fifth Assessment Report: Climate Change 2013*, eds Stocker TF, et al. (Cambridge Univ Press, Cambridge, UK), pp 1031, 1054–1055.
- Clark PU, et al. (2016) Consequences of twenty-first-century policy for multi-millennial climate and sea-level change. *Nat Clim Chang* 6:360–369.
- Schewe J, et al. (2014) Multimodel assessment of water scarcity under climate change. *Proc Natl Acad Sci USA* 111:3245–3250.
- Peñuelas J, et al. (2013) Evidence of current impact of climate change on life: A walk from genes to the biosphere. *Glob Change Biol* 19:2303–2338.
- Dirzo R, et al. (2014) Defaunation in the Anthropocene. *Science* 345:401–406.
- Myers SS, et al. (2013) Human health impacts of ecosystem alteration. *Proc Natl Acad Sci USA* 110:18753–18760.
- Mahony CR, MacKenzie WH, Aitken SN (2018) Novel climates: Trajectories of climate change beyond the boundaries of British Columbia's forest management knowledge system. *For Ecol Manage* 410:35–47.
- Milly PCD, et al. (2008) Climate change. Stationarity is dead: Whither water management? *Science* 319:573–574.
- Diffenbaugh NS, et al. (2017) Quantifying the influence of global warming on unprecedented extreme climate events. *Proc Natl Acad Sci USA* 114:4881–4886.
- Steffen W, et al. (2018) Trajectories of the Earth system in the Anthropocene. *Proc Natl Acad Sci USA* 115:8252–8259.
- Rockström J, et al. (2009) A safe operating space for humanity. *Nature* 461:472–475.
- Radeloff VC, et al. (2015) The rise of novelty in ecosystems. *Ecol Appl* 25:2051–2068.
- Williams JW, Jackson ST, Kutzbach JE (2007) Projected distributions of novel and disappearing climates by 2100 AD. *Proc Natl Acad Sci USA* 104:5738–5742.
- Mahony CR, Cannon AJ, Wang T, Aitken SN (2017) A closer look at novel climates: New methods and insights at continental to landscape scales. *Glob Change Biol* 23:3934–3955.
- Mora C, et al. (2013) The projected timing of climate departure from recent variability. *Nature* 502:183–187.
- Hawkins E, et al. (2014) Uncertainties in the timing of unprecedented climates. *Nature* 511:E3–E5.
- Diffenbaugh NS, Charland A (2016) Probability of emergence of novel temperature regimes at different levels of cumulative carbon emissions. *Front Ecol Environ* 14:418–423.
- Hansen J, et al. (1981) Climate impact of increasing atmospheric carbon dioxide. *Science* 213:957–966.
- Crowley TJ (1990) Are there any satisfactory geologic analogs for a future greenhouse warming? *J Clim* 3:1282–1292.
- Zachos J, Pagani M, Sloan L, Thomas E, Billups K (2001) Trends, rhythms, and aberrations in global climate 65 Ma to present. *Science* 292:686–693.
- Pagani M, Zachos JC, Freeman KH, Tipple B, Bohaty S (2005) Marked decline in atmospheric carbon dioxide concentrations during the Paleogene. *Science* 309:600–603.
- Caballero R, Huber M (2013) State-dependent climate sensitivity in past warm climates and its implications for future climate projections. *Proc Natl Acad Sci USA* 110:14162–14167.
- Anagnostou E, et al. (2016) Changing atmospheric CO₂ concentration was the primary driver of early Cenozoic climate. *Nature* 533:380–384.
- Pagani M, Liu Z, Lariviere J, Ravelo AC (2010) High Earth-system climate sensitivity determined from Pliocene carbon dioxide concentrations. *Nat Geosci* 3:27–30.
- Haywood AM, et al. (2013) Large-scale features of Pliocene climate: Results from the Pliocene Model Intercomparison Project. *Clim Past* 9:191–209.
- Fischer H, et al. (2018) Palaeoclimate constraints on the impact of 2 °C anthropogenic warming and beyond. *Nat Geosci* 11:474–485.
- Otto-Bliesner BL, et al. (2017) Two interglacials: Scientific objectives and experimental designs for CMIP6 and PMIP4 Holocene and last interglacial simulations. *Geosci Model Dev* 10:3979–4003.
- Marcott SA, Shakun JD, Clark PU, Mix AC (2013) A reconstruction of regional and global temperature for the past 11,300 years. *Science* 339:1198–1201.
- Rohling EJ, et al. (2018) Comparing climate sensitivity, past and present. *Annu Rev Mar Sci* 10:261–288.
- Braconnot P, et al. (2012) Evaluation of climate models using palaeoclimatic data. *Nat Clim Chang* 2:417–424.
- Lunt DJ, et al. (2017) The DeepMIP contribution to PMIP4: Experimental design for model simulations of the EECO, PETM, and pre-PETM (version 1.0). *Geosci Model Dev* 10:889–901.
- Lunt DJ, et al. (2012) A model-data comparison for a multi-model ensemble of early Eocene atmosphere-ocean simulations: EoMIP. *Clim Past* 8:1717–1736.
- Carmichael MJ, et al. (2016) A model-model and data-model comparison for the early Eocene hydrological cycle. *Clim Past* 12:455–481.
- Ruddiman WF (2013) The Anthropocene. *Annu Rev Earth Planet Sci* 41:45–68.
- Schlebusch CM, et al. (2017) Southern African ancient genomes estimate modern human divergence to 350,000 to 260,000 years ago. *Science* 358:652–655.
- Steffen W, et al. (2015) Sustainability. Planetary boundaries: Guiding human development on a changing planet. *Science* 347:1259855.
- Kidwell SM (2015) Biology in the Anthropocene: Challenges and insights from young fossil records. *Proc Natl Acad Sci USA* 112:4922–4929.
- Walther GR, et al. (2002) Ecological responses to recent climate change. *Nature* 416:389–395.
- Edwards EJ, et al.; C4 Grasses Consortium (2010) The origins of C4 grasslands: Integrating evolutionary and ecosystem science. *Science* 328:587–591.
- Svenning J-C (2003) Deterministic Plio-Pleistocene extinctions in the European cool-temperate tree flora. *Ecol Lett* 6:646–653.
- Williams JW, Burke KD (2019) Past abrupt changes in climate and terrestrial ecosystems. *Biodiversity and Climate Change: Transforming the Biosphere*, eds Lovejoy TE, Hannah L (Yale Univ Press, New Haven, CT), pp 128–141.
- Trenberth KE, Fasullo JT, Shepherd TG (2015) Attribution of climate extreme events. *Nat Clim Chang* 5:725–730.
- Haywood AM, et al. (2016) The Pliocene Model Intercomparison Project (PlioceneMIP) phase 2: Scientific objectives and experimental design. *Clim Past* 12:663–675.
- Taylor KE, Stouffer RJ, Meehl GA (2012) An overview of CMIP5 and the experiment design. *Bull Am Meteorol Soc* 93:485–498.
- Schmidt GA, et al. (2014) Using palaeo-climate comparisons to constrain future projections in CMIP5. *Clim Past* 10:221–250.
- Meinshausen M, et al. (2011) The RCP greenhouse gas concentrations and their extensions from 1765 to 2300. *Clim Change* 109:213–241.
- Thomson AM, et al. (2011) RCP4.5: A pathway for stabilization of radiative forcing by 2100. *Clim Change* 109:77–94.
- Riahi K, et al. (2011) RCP 8.5-A scenario of comparatively high greenhouse gas emissions. *Clim Change* 109:33–57.
- Harris I, Jones PD, Osborn TJ, Lister DH (2014) Updated high-resolution grids of monthly climatic observations—The CRU TS3.10 Dataset. *Int J Climatol* 34:623–642.
- Pearson RG, Dawson TP (2003) Predicting the impacts of climate change on the distribution of species: Are bioclimate envelope models useful? *Glob Ecol Biogeogr* 12:361–371.
- Zachos JC, Dickens GR, Zeebe RE (2008) An early Cenozoic perspective on greenhouse warming and carbon-cycle dynamics. *Nature* 451:279–283.
- Lisiecki LE, Raymo ME (2005) A Pliocene-Pleistocene stack of 57 globally distributed benthic $\delta^{18}\text{O}$ records. *Paleoceanography* 20:PA1003.
- Jouzel J, et al. (2007) Orbital and millennial Antarctic climate variability over the past 800,000 years. *Science* 317:793–796.
- Andersen KK, et al.; North Greenland Ice Core Project members (2004) High-resolution record of Northern Hemisphere climate extending into the last interglacial period. *Nature* 431:147–151.
- Morice CP, Kennedy JJ, Rayner NA, Jones PD (2012) Quantifying uncertainties in global and regional temperature change using an ensemble of observational estimates: The HadCRUT4 data set. *J Geophys Res Atmos* 117:D08101.
- Hansen J, Sato M, Russell G, Kharecha P (2013) Climate sensitivity, sea level and atmospheric carbon dioxide. *Philos Trans A Math Phys Eng Sci* 371:20120294.
- Moritz C, Agudo R (2013) The future of species under climate change: Resilience or decline? *Science* 341:504–508.